ISSN 2004-2965 Energy Proceedings, Vol. 18, 2021

International Conference on Applied Energy 2021
Nov. 29 - Dec. 5, 2021, Thailand/Virtual
Paper ID: 699

Dean Instability Phenomenon and its Effect on Heat Transfer in Sinusoidal Channel

Xueling Liu [1,2*], Yuguo Fu [1,2], Jiansheng Wang [1], Jintao Niu [1,2]

1 Key Laboratory of Efficient Utilization of Low and Medium Grade Energy, MOE, School of Mechanical Engineering, Tianjin University, Tianjin, 300354, P. R. China

2 Geothermal Research & Training Center, Tianjin University, Tianjin, 300354, P. R. China

ABSTRACT

The curvature and bending direction of a sinusoidal channel show periodic changes, so its internal flow and heat transfer characteristics are more complex. In this paper, Direct Numerical Simulation method is used to calculate the square sinusoidal channels with different cross-sectional ratios. The results show that in the laminar flow range, the Dean vortex loses stability when the Reynolds number increases to a certain value, which is manifested as random fluctuations of the Dean vortex with time and space. This state is called Dean instability phenomenon, and the critical Reynolds number corresponding to 1:2 cross-sectional ratio of the sinusoidal channel is determined by using the helicity discrimination method. In addition, by comparing the heat transfer characteristics of the channels in the two states, it is found that after reaching the Dean instability state, the heat transfer enhancement caused by the Dean vortex is not limited to a fixed position, which has significant implications for enhancing the heat transfer capacity and reducing the wall temperature difference.

Keywords: Heat exchanger, Dean instability phenomenon, Critical Reynolds number, Heat transfer characteristics

NONMENCLATURE

Symbols	
a	Height of cross section(mm)
a*	Dimensionless height = a/Dh
b	Width of cross section(mm)
b*	Dimensionless width = b/Dh
D	Diameter of curvature(mm)
Dh	Hydraulic diameter(mm)
h	Heat transfer coefficient(W/ m^2 • K)
H	Helicity(m/s^2)
Nu	Nusselt number
Re	Reynolds number
V	Velocity(m/s)
y*	Dimensionless width coordinate= y/b
α	Aspect Ratio (a/b)
θ	Angle
λ	Thermal conductivity(W/m • K)
μ	Dynamic viscosity(N • s/m^2)
ρ	Density(kg/m^3)

1. INTRODUCTION

The optimal design of heat exchangers is of great significance for improving the energy utilization of equipment and alleviating the problems of energy shortage and waste heat in chemical power, aviation power and other industrial fields. Sinusoidal structure is widely used in various heat exchangers because of its excellent heat transfer characteristics and good spatial stacking. Compared with methods such as using micro and nano fluids[1,2], adding disturbing units in the channel[3,4], curved channel is a convenient and effective way to enhance heat transfer.

In terms of micro heat sink design, Ji-Feng Zhu et al.[5] investigated the heat transfer performance of left-right and up-down wavy microchannel heat sinks. By comparing the thermal resistance and maximum temperature difference of the two heat sinks under different wave amplitude and wavelength, it was found that the up-down wavy microchannel heat sinks were more advantageous under the same conditions. Wang et al.[6] proposed a double-layer wavy microchannel and used a porous rib structure for the walls. The results of the study showed that the porous structure greatly reduced the pumping power of the heat sink. In the study of heat exchangers, the thermal properties of steam-air in a sinusoidal bellows condensation wall were investigated using numerical calculations by Xuebo Dong et al.[7] Geometric parameter designs were proposed for parameters such as wavelength and wave amplitude of the bellows condensation wall. Samaneh Arman et al.[8] investigated the effect of Reynolds number, wave amplitude and wavelength on heat transfer in a bellows with circular cross-section using numerical calculations. The results show that the thermal performance of the bellows is directly proportional to Reynolds number and wave amplitude and inversely proportional to wavelength in the studied range.

The heat transfer performance of sinusoidal structure cannot be studied without the flow characteristics of the secondary flow. The laminar flow of a Newtonian fluid in a 180° curved channel was studied experimentally and numerically by H. Fellouah et al[9], where an instability criterion based on the radial gradient of the axial velocity was defined, and the relationship between the critical Dean number and the aspect ratio and curvature of the duct was determined. The development of additional counter-rotating Dean vortexes was also observed. Li Yalin et al.[10] investigated experimentally and numerically the fully developed turbulent flow of water in a rectangular cross-section with 120° bend, proposed a new criterion based on the vortex core velocity, and observed entrained Dean vortices near the outlet location of the pipe. The motion and heat transfer processes of Dean vortices in curved channels were studied numerically by Tilak et al[11], using helicity and wall pressure gradient methods to determine the key phenomena of hydrodynamic instability.

There are many previous studies on Dean instability in single bend direction channel. However, the Dean instability in the sinusoidal channel is completely different from it. This is due to the alternating changes in the curvature of the sinusoidal structure. Therefore, this paper investigates the Dean instability phenomenon in sinusoidal structures by computational fluid dynamics (CFD) method and further explores the changes of heat transfer characteristics caused by it.

2. PHYSICAL MODEL AND NUMERICAL PROCESS

2.1 Physical model

As shown in Fig. 1, the sine function $y = A\sin(\omega x + \phi)$ is used as the channel center curve, in which A and ω is taken as 1, and ϕ is taken 0. The width of the channel is b and the height is a, and L is represented the length of channel. The location of the cross-section is indicated by using the channel degree θ. For example, 0° cross-section is the inlet and 360° cross-section is the outlet. The channel parameters are dimensionless, with b* and a* representing the dimensionless width and height, respectively.

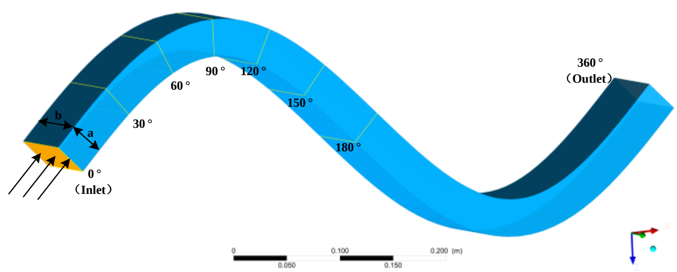

Fig. 1. Sinusoidal Channel model

2.2 Governing equations

Continuity equation

$$\nabla(\vec{V}) = 0 \tag{1}$$

Momentum equations

$$\rho\frac{\partial\vec{V}}{\partial t} + \vec{V}\bullet\nabla(\rho\vec{V}) = -\nabla p + \mu\nabla^2\vec{V} + \vec{F_c} \tag{2}$$

Energy equation

$$\rho\frac{\partial T}{\partial t} + \vec{V}\bullet\nabla(\rho\vec{V}\,T) = \frac{\lambda}{c_p}\nabla^2 T \tag{3}$$

Besides, some dimensional numbers and parameters are used to describe the channel flow and heat transfer characteristics.

Reynolds number

$$\mathrm{Re} = \rho V D_h / \mu \tag{4}$$

Dean number

$$D_n = \mathrm{Re} \times (D_h / D)^{0.5} \tag{5}$$

Nusselt number

$$Nu = hD_h / \lambda \tag{6}$$

Helicity

$$H = u\left(\frac{\partial w}{\partial y} - \frac{\partial v}{\partial z}\right) + v\left(\frac{\partial u}{\partial z} - \frac{\partial w}{\partial x}\right) + w\left(\frac{\partial v}{\partial x} - \frac{\partial u}{\partial y}\right) \tag{7}$$

In the course of numerical calculations, periodic boundary conditions are used for the outlet and inlet, and no-slip conditions are used for the walls. When heating is present, the inlet fluid temperature is set to 300 K, while a 400 K Dirichlet condition is applied for the wall temperature. The SIMPLE algorithm is used to couple velocity and pressure, while a second-order implicit discretization is used for time.

2.3 Grid independence test

To ensure that the number of grids has no effect on the calculation results, the grid independence was verified by using the grids in Table 1. From the calculation results, it can be seen that the wall friction coefficient does not show correlation with the number of grids when the number of grids is larger than Mesh 2. Therefore, the number of grids is considered according to the Nusselt number. The Richardson extrapolation method was used to calculate Mesh 3,4,5,6, and the Richardson coefficients R of them is less than 1. However, using a smaller number of grids can save computational time while ensuring accuracy. Therefore, Mesh 5 is chosen for subsequent calculations.

Table 1. Grid independence test for α =1:2 and Re=322.73

Mesh	grid number	Nusselt number	skin friction coefficient
Mesh 1	25920	3.266	0.065
Mesh 2	87552	3.235	0.069
Mesh 3	156600	3.207	0.069
Mesh 4	290304	3.142	0.070
Mesh 5	681984	3.116	0.070
Mesh 6	2187936	3.094	0.069

$$\varepsilon_{43}=Nu_4\text{-}Nu_3=-0.065 \tag{8}$$

$$\varepsilon_{54}=Nu_5\text{-}Nu_4=-0.026 \tag{9}$$

$$\varepsilon_{65}=Nu_6\text{-}Nu_5=-0.022 \tag{10}$$

$$R_{3,4,5}=\frac{\varepsilon_{54}}{\varepsilon_{43}}=0.400 \tag{11}$$

$$R_{4,5,6}=\frac{\varepsilon_{65}}{\varepsilon_{54}}=0.864 \tag{12}$$

$$0<R_{3,4,5}<R_{4,5,6}<1 \tag{13}$$

3. RESULT AND DISCUSSION

3.1 Dean instability phenomenon

In the past, the Dean instability in the bend was defined as the appearance of inner wall Dean vortex or the generation of split Dean vortex. However, since the sinusoidal channel has two opposite bending directions in a period, it is easy to generate inner wall Dean vortex and split Dean vortex. At the same time, these two instabilities do not have a significant effect on the sinusoidal channel heat transfer, so this paper redefines the Dean instability as the loss of symmetry of the cross-sectional Dean vortexes. The results show that in the Dean steady state, the main flow characteristics in the channel do not change with time, and the legacy Dean vortexes with less intensity fluctuations show symmetry and periodicity, so the heat transfer characteristics are fixed. When the flow becomes unsteady, the Dean vortex is in a disordered fluctuation state, which causes fluctuations in the local Nusselt number at the wall.

3.2 Detection method of Helicity

According to previous research literature, it is proved that helicity has good accuracy in determining the Dean instability in the laminar flow state [11]. At the same time, helicity has good three-dimensional display characteristics. Therefore, helicity is chosen as the display of the flow state in the sinusoidal channel.

Table 2. shows the maximum and minimum values of helicity in the channel at three Reynolds numbers. These three Reynolds numbers correspond to steady state, critical state and Dean instable state respectively. In order to accurately represent the flow state of the Dean vortex in the channel, it is necessary to select the appropriate helicity equivalent value. When a large value of helicity equivalent is selected, the flow details will be missed. And when a small value is chosen, the main structure of the Dean vortex cannot be clarified. Therefore, based on the calculation results, 10% of the maximum and minimum helicity values are chosen as the values of the iso-surface.

Fig. 2 shows the helicity iso-surface. It can be seen that when the Reynolds number is 322.73, the channel helicity shows a symmetric structure. As the Reynolds number increases to 451.82, the channel shows a local asymmetric structure. When the Reynolds number continues to increase to 645.45, the channel shows a strong instability.

Table 2. The Helicity of three channel

Re	H_{max}	H_{min}	$H_{iso\text{-}red}$	$H_{iso\text{-}blue}$
322.73	2.075	-2.076	0.207	-0.208
451.82	12.097	-8.872	1.210	-0.887
645.45	4.344	-4.218	0.434	-0.422

To further investigate the effect of Reynolds number on Dean instability, Fig. 3 and Fig. 4 show the helicity of the channel 90° cross-section at different

Reynolds numbers. It can be seen that the centrifugal force not only strengthens the main Dean vortexes near the left and right walls, but also enhances the legacy Dean vortexes in the center of the channel when in the steady state. When transitioning to the unsteady state, the main Dean vortex has been deformed, while the legacy Dean vortex has completely lost its original state.

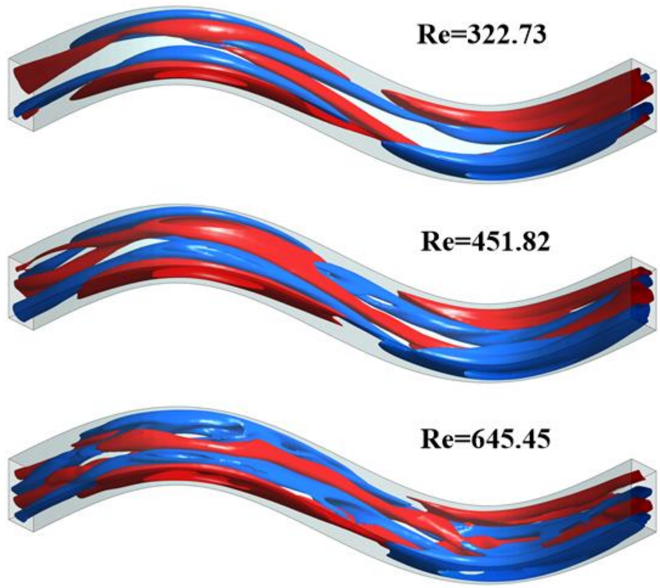

Fig. 2. Iso-surface of Helicity for 1:2 cross-sectional sinusoidal channel

Velocity and helicity clouds for different cross-sections at critical Reynolds number are displayed in Fig. 5. Combining multiple time results, it is found that the asymmetric structures usually arise in the range of 0-30°, 150-210° and 330-360°. This is caused by two reasons: One is the change of the bending direction at these locations, which makes the reversal of the direction of the Dean vortex rotation in the channel. The other reason is that the small curvature makes the fluid susceptible to flow instability because of the weak flow constraints which is caused by the weak centrifugal forces exerted on the fluid. The Dean instability phenomenon is weaker at the location of large curvature. This is because the stronger centrifugal force intensifies the main Dean vortex, and the asymmetric structure receives a certain degree of restraint. However, it can be seen that the asymmetry appears at positions of higher curvature at some moments, which is because the asymmetric structure advances with the main flow direction.

Sinusoidal channels with 1:1, 1:3, 1:4, 1:5 and 1:6 cross-sectional ratios are investigated using the same numerical calculation method. The results show that for the channels with small cross-sectional ratios, the Dean instability is manifested as a difference in the shape of the Dean vortexes. For channels with large cross-sectional ratios, the Dean vortexes exist in the form of multiple pairs and small intensity due to the channel height limitation. The instability in this case is caused by the asymmetry of the number of Dean vortexes.

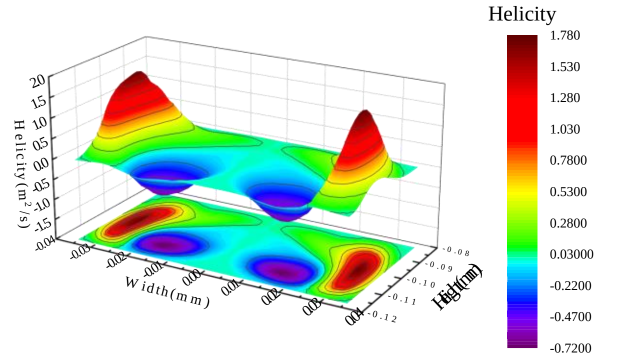

Fig. 3. Helicity of section 90° for α = 1:2 and Re = 322.73

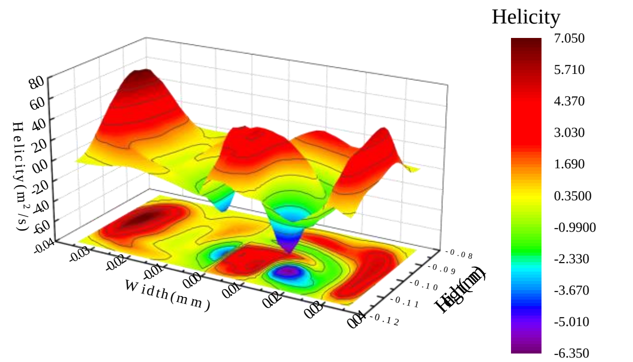

Fig. 4. Helicity of section 90° or α = 1:2 and Re = 645.45

In addition to the helicity method, there are several other methods to determine the Dean instability phenomenon. A brief introduction is given here. The inner wall surface pressure gradient is a common method used in previous experiments and numerical calculations. However, because of the distance of the Dean vortex from the wall, it causes the Dean instability to need to exceed a threshold value before it can be manifested in the pressure gradient. Therefore, this method is less accurate. The radial velocity gradient is a more accurate method. Two straight lines at symmetric locations on the cross-section are selected and their radial velocity gradients are compared. But there is no clear method for the selection of straight lines position, and which directly affects the judgment result. Comparing the position of the vortex center is also a method to judge the instability. This method can judge not only the asymmetry of the Dean vortex position, but also the asymmetry of the number of Dean vortexes. However, it cannot show the intensity of the Dean vortex instability.

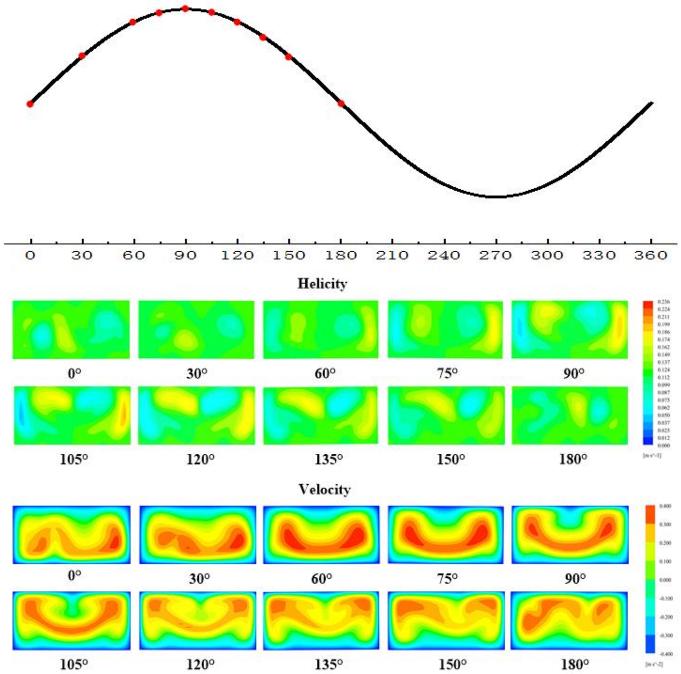

Fig. 5. Different cross-sectional velocity and helicity for Re = 451.82

3.3 The effect of Dean instability on heat transfer

Fig. 6 shows the wall Nusselt number cloud diagram for 30 s, 35 s and 40 s at three Reynolds numbers.

When the Reynolds number is 322.73, there are two Nusselt number peaks corresponding to the left and right at the outer wall near the 90° cross-section, which is the best position for heat transfer in the sinusoidal channel. The heat transfer capacity at the center of the 150° position is relatively better around it, which is caused by the fluctuation of the legacy Dean vortexes. However, its Nusselt number is small compared to that of 90° position. The other positions of the channel have a weaker heat transfer capacity.

When the Reynolds number is 451.82, two heat transfer peaks are existed. This is because the loss of symmetry of the Dean vortexes is the beginning of the Dean instability, and it needs to reach a certain strength before it affects the heat transfer. It can be seen that the heat transfer on right side is stronger than the left side at 40 s.

When the Reynolds number reaches 645.45, the Reynolds number has exceeded the critical Reynolds number and reached the strong instability. From the Fig. 6, it can be seen that the peak Nusselt number and the corresponding position are different in the three moments. The local Nusselt number variation caused by the destabilization of the Dean vortex.

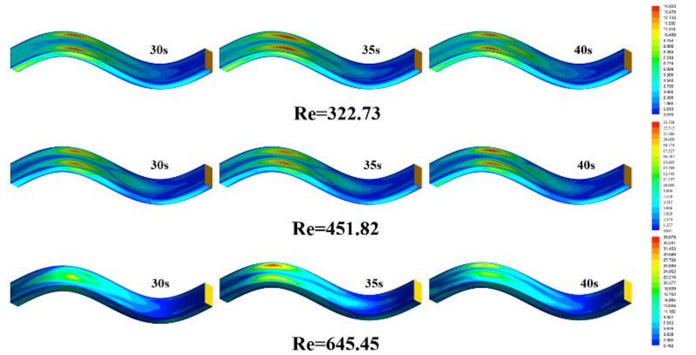

Fig. 6. Surface Nusselt number for 1:2 cross-sectional sinusoidal channel

Fig. 7 shows the local Nusselt number for the 90° outer wall. Due to the fluctuation of the main Dean vortex, which caused by the Dean instability phenomenon, the local Nusselt number at the central position changes significantly with time. Compared with the low local Nusselt number at the center position at steady state, its heat transfer capacity is improved considerably. In addition to the temporal fluctuations at the fixed position, the Dean instability phenomenon also causes heat transfer enhancement at other spatial positions, as shown in Fig. 6. This fluctuation reduces the difference of heat transfer capacity at different locations and facilitates the enhancement of the channel heat transfer capacity.

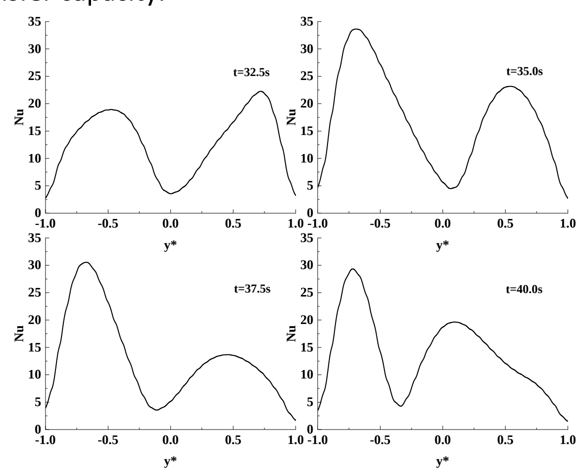

Fig. 7. Local Nusselt number of 90° outer wall for α = 1:2 and Re = 645.45

4. CONCLUSIONS

In this paper, flow and heat transfer characteristics of sinusoidal channel are investigated by using numerical calculation method, and the conclusions are shown as follow.

1. The previous definition of the Dean instability phenomenon is not meaningful in sinusoidal channels. Therefore, the beginning of the Dean instability is redefined as the loss of symmetry of the Dean vortexes

in the channel, and the critical Reynolds number of the sinusoidal channel with 1:2 cross section is determined.

2. The flow characteristics of the Dean vortex are studied using the helicity method. The wall pressure gradient, radial velocity gradient and vortex center methods are also summarized. It is finally found that helicity has high accuracy in the laminar flow condition.

3. The effect of the Dean instability phenomenon on the surface Nusselt number is investigated. It is found that the local Nusselt number fluctuates with the fluctuation of the Dean vortex in the unsteady state, which reduces the difference in the heat transfer capacity of the channel walls.

REFERENCE

[1]İlhan B, Ertürk H. Experimental characterization of laminar forced convection of hBN-water nanofluid in circular pipe. Int J Heat Mass Tran 2017;111:500-507.

[2]Fsadni AM, Whitty JPM, Stables MA, Adeniyi AA. Numerical study on turbulent heat transfer and pressure drop characteristics of a helically coiled hybrid rectangular-circular tube heat exchanger with Al2O3-water nanofluids. Appl Therm Eng 2017;114:466-483.

[3]Guo A, Wang L. Parametrization of secondary flow intensity for laminar forced convection in twisted elliptical tube and derivation of loss coefficient and Nusselt number correlations by numerical analysis. Int J Therm Sci 2020;155:106425.

[4]Shi H, Zhao Y, Liu Z. Numerical investigation of the secondary flow effect of lateral structure of micromixing channel on laminar flow. Sensors and Actuators B: Chemical 2020;321:128503.

[5]Zhu J, Li X, Wang S, Yang Y, Wang X. Performance comparison of wavy microchannel heat sinks with wavy bottom rib and side rib designs. Int J Therm Sci 2019;146:106068.

[6]Wang S, Chen L, Zhang B, Yang Y, Wang X. A new design of double-layered microchannel heat sinks with wavy microchannels and porous-ribs. J Therm Anal Calorim 2020;141:547-558.

[7]Dong X, Chen W, Cheng Q, Liu Y, Dai H. Numerical analysis of thermal-hydraulic characteristics of steam-air condensation in vertical sinusoidal corrugated tubes. Int J Heat Mass Tran 2021;164:120558.

[8]Arman S, Hassanzadeh R. Effects of the geometric parameters on the thermal-hydraulic performance of the wavy tubes. Int Commun Heat Mass 2018;96:27-36.

[9]Fellouah H, Castelain C, Ould El Moctar A, Peerhossaini H. A criterion for detection of the onset of Dean instability in Newtonian fluids. European Journal of Mechanics - B/Fluids 2006;25:505-531.

[10]Li Y, Wang X, Zhou B, Yuan S, Tan SK. Dean instability and secondary flow structure in curved rectangular ducts. Int J Heat Fluid Fl 2017;68:189-202.

[11]Chandratilleke TT, Nadim N, Narayanaswamy R. Vortex structure-based analysis of laminar flow behaviour and thermal characteristics in curved ducts. Int J Therm Sci 2012;59:75-86.